Chaos, Solitons and Fractals 168 (2023) 113089

Contents lists available at ScienceDirect

Chaos, Solitons and Fractals

journal homepage: www.elsevier.com/locate/chaos

Stabilisation of spatially periodic states by non-Hermitian potentials

Salim B. Ivars [a,*], Muriel Botey [a], Ramon Herrero [a], Kestutis Staliunas [a,b,c]

[a] Departament de Física, Universitat Politècnica de Catalunya (UPC), Rambla Sant Nebridi 22, 08222, Terrassa, Barcelona, Catalonia, Spain
[b] Institució Catalana de Recerca i Estudis Avançats (ICREA), Passeig Lluís Companys 23, E-08010, Barcelona, Spain
[c] Vilnius University, Faculty of Physics, Laser Research Center, Sauletekio Ave. 10, Vilnius, Lithuania

ARTICLE INFO

Keywords:
Complex Ginzburg Landau equation
Stabilisation
Periodic solutions
Non-Hermitian potential
VCSEL
Fractional

ABSTRACT

We uncover new families of stable periodic solutions by the introduction of non-Hermitian potentials in the universal complex Ginzburg–Landau equation. We perform a comprehensive analysis on the dynamics and stability of the system by determining and following these new solutions for a one-dimensional system, and demonstrate that the results hold for higher spatial dimensions and for the corresponding complex Ginzburg–Landau fractional order equation. We prove the robustness of the stabilisation within a broad range in parameter space. The universality of the CGLE allows extending these results to different actual systems described by other specific models. In particular, we provide results on the stabilisation for Vertical Cavity Surface Emitting Lasers.

1. Introduction

The Complex Ginzburg–Landau Equation (CGLE) is a universal mathematical model for pattern formation and turbulence in extended physical systems. It can be derived as an order parameter equation to describe a variety of phenomena in different contexts ranging from superconductivity, superfluidity, nonlinear wave dynamics, second-order phase transitions, liquid crystals to Bose–Einstein condensation or strings theory [1]. Combining its universal character to the simplicity of the model, the CGLE has become one of the most studied non-linear equations in physics, and applied mathematics [2–5].

Particularly in optics, it describes light propagation in nonlinear dissipative media, therefore including a variety of nonlinear systems like ring cavities [5–7], fibre or semiconductor lasers [8,9] and ultra-fast optics [10].

The CGLE is known to support different types of solutions, either being localised solutions [11–15], periodic in space and time [16], periodic in space [5,17], quasi-periodic [13] or vortices [18–21], yet the search of new solutions is constantly retrieving attention [22–24]. Some of these solutions have been found to be stable under certain conditions, either for weak self-focusing [5,25], considering higher order terms and diffusion [14,15,26,27], or for the defocusing case [26]. For self-focusing nonlinearity, modulation instability (MI) of the homogeneous solution, leads to turbulent regimes for a wide range of parameters [1,28].

The control of turbulence in dynamical systems is a significant problem, not only for the fundamental understanding of the physical mechanism behind turbulence but also for its practical consequences. Turbulence is present in a wide variety of physical systems [29,30]. Broad aspect-ratio laser sources are a paradigmatic example among optical sources, since turbulence represents one of the main inconveniences when increasing emission power. Yet, the need for high-power laser sources for practical applications has increased in recent years. In particular, the affordable, compact, and integrable Vertical External-Cavity Surface Emitting Lasers (VCSELs) or Edge-Emitting Lasers (EELs), suffer from spatio-temporal instabilities that severely compromise their beam quality [31]. Some efficient techniques for the control of turbulence consider a global delayed feedback on the system [32] or the effect of a gradient [33]. Recently, new methods based on the introduction of Hermitian (real) periodic potentials have proven to suppress MI [34]. Besides, non-Hermitian (complex) Photonics has emerged as an attractive platform to uncover unconventional effects. [35–38]. In particular, asymmetries in the coupling of the spatio-temporal modes allow the modification of the excitation cascade [39]. Also, for the particular class of Parity Time (PT)-symmetric systems, a particular example of non-Hermitian potentials, the existence of solitons, defect states, vortices, and other structures has been studied [40]. Such localised structures and their non-linear dynamics have also been addressed, showing that these solitons can be robust and stable [41].

In this work, we face the control of turbulence in a dynamical system under a different approach. We directly stabilise specific periodic stationary solutions of the CGLE by the introduction of a non-Hermitian

* Corresponding author.
E-mail address: salim.benadouda@upc.edu (S.B. Ivars).

https://doi.org/10.1016/j.chaos.2022.113089
Received 3 October 2022; Received in revised form 17 November 2022; Accepted 27 December 2022
Available online 13 January 2023

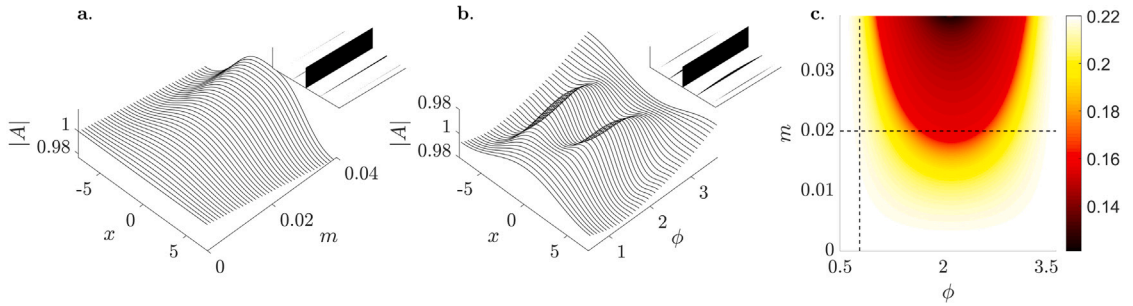

Fig. 1. Effect of the non-Hermitian potential on the homogeneous solution. Amplitude of the spatial profile of the modulation for: **a.** a fixed value of $\phi = \pi/4$, as a function of m; and **b.** for a fixed $m = 0.01$ as a function on ϕ. Insets in both plots correspond to the Fourier transform as a function of m and ϕ respectively. **c.** Growth rate of the nearly homogeneous solution as a function of the potential parameters, for $L = 15$. Vertical and horizontal dashed lines correspond to the situations depicted in **a.** and **b.**, respectively. $\alpha = 0.7$ for all plots.

harmonic potential to turn these states into attractors. When these states present a large enough attraction basin, they may be easily reached via the MI of the system

We first show the effect of the proposed potential on the simplest solution: the homogeneous state. Next, we uncover families of periodic stationary solutions of the CGLE as candidates for stabilisation; and provide a comprehensive numerical analysis of the stability regimes in the parameter space. Then, we extend the method to higher spatial dimensions; indeed, 2D models allow describing the general dynamics of most lasers. In turn, fractional equations have attracted recent interest in various areas of physics. Thus, we further study the introduction of a non-Hermitian potential in the fractional CGLE, finding examples of stabilisation for various fractional orders. Finally, as an example, we show an application on a more specific model describing actual systems, in particular VCSELs.

2. Model and results

For the study we consider the CGLE that models the evolution of a field envelope $A(\mathbf{r}, t)$. In one of its possible forms, it reads:

$$\frac{\partial A}{\partial t} = i\nabla^2 A + (1 - i\alpha)\left(1 - |A|^2\right)A + V(\mathbf{r})A, \tag{1}$$

where $A(\mathbf{r}, t)$ is a complex function of time, t, and space, $\mathbf{r}$, and α is the self-focusing coefficient. The potential $V(\mathbf{r})$ is a complex-valued function that, in the case of an optical system, would represent refractive index and gain or loss spatial modulations that can be implemented in optics with present technological techniques [38]. Without loss of generality, the homogeneous gain and dispersion coefficients may be normalised to unity.

In the absence of potential, for $V = 0$, the most well-known and studied non homogeneous solutions are simple stable periodic solutions for small values of the self-focusing coefficient and localised states. Here, we enlarge the study to a more general class of periodic solutions.

We introduce a periodic modulation in the form:

$$V(x) = m\cos\left(\frac{2\pi x}{L}\right)e^{-i\phi}. \tag{2}$$

The potential depends on three parameters: the spatial period, L, the amplitude of the modulation, m, and the ratio between the real and imaginary part of the modulation, ϕ. This exponential has a periodicity of 2π and shows two different configurations. For $0 < \phi < \pi/2$ and $\pi < \phi < 3\pi/2$ we see that the modulation is in-phase, meaning that the real and imaginary parts of the potential have the same sign. Contrary, for $\pi/2 < \phi < \pi$ and $3\pi/2 < \phi < 2\pi$ we have counterphase modulation, meaning that the real and imaginary parts of the potential have opposite sign. Note that since the potential is harmonic, the resulting periodicity is of π with respect to ϕ.

To address the effect of the modulation on the system stability, we first assess the effect on the homogeneous solution of the CGLE, $|A| = 1$. We assume a fixed periodicity L, and investigate the variations of the homogeneous solution with the introduction of the modulation. We observe that for $\phi = \pi/4$ the potential slowly modulates the solution and the first harmonics slowly appear, see Fig. 1**a.** Comparing this behaviour to the scan of ϕ with fixed modulation amplitude m (Fig. 1**b.**) we appreciate the sharper effect on the solution of the last, that is, the second harmonics appear faster in terms of modulation amplitude. In both cases, there is a predominance of the central harmonic (the homogeneous part). We apply linear stability analysis to the modulated solution, and map the stability in the (ϕ, m) parameter space, see Fig. 1**c.** We note that, for all values of ϕ, the largest real part of the Lyapunov exponents, the growth rate, decreases with m (see methods section). Such spatially periodic potentials induce an effective diffusion on a large spatial scale that triggers the stabilisation of the system. However, for larger values of m, the solution disappears through a saddle–node (SN) bifurcation. Therefore, the proposed method does not stabilise slightly modulated solutions smoothly arising from the homogeneous state.

Yet, our study is aimed at determining steady periodical solutions of the CGLE susceptible to be stabilised. Thus, the study is next focused on determining steady solutions of the unmodulated system, *i.e.* solutions of Eq. (1) in the form $A(\mathbf{r}, t) = A(\mathbf{r})\exp(i\omega t)$, being ω the characteristic frequency of the solution. We are able to localise and follow such states independently of their stability in the parameter space by using a modified Newton method described in [42].

The stationary states can be characterised by their norm $N_A \equiv 1/L\int_{-L/2}^{L/2}|A(x)|\,dx$ and their spatial period, L, see Fig. 2 showing the branches of solutions that will be studied below. First, we note that for small values of L, there are two types of solutions. On the one hand, the trivial and homogeneous solution $|A| = 1$, corresponding to the upper branch in Fig. 2**a.** The spatial profile, for small values of L is provided in Fig. 2**b.** under the label (a). On the other hand, still for small L, an almost sinusoidal solution exists with a dominant single spatial frequency. This solution corresponds to the lower branch in Fig. 2**a.** and its profile is plotted in Fig. 2**c.** labelled as (d). For this last case, we have analytically proven that its corresponding characteristic frequency ω tends to infinity when L tends to zero and has a quadratic growth on $1/L$. Increasing L, the two families of solutions become connected by new branches of intermediate solutions arising from the first two ones. Note, for example, the similarity in the profiles of (c) in Fig. 2**b.** and (g) in Fig. 2**c.**, both deriving from the homogeneous solution and the last connected to (d). These states correspond to Turing-like patterns with different number of rolls. Further increasing the spatial periodicity, these rolls develop to the coexistence of different solitons. From the branch starting at point (d), two extra bifurcation points (e) and (f) leading to new classes of periodic solutions. Finally, the inset on Fig. 2**a.** zooms in the branches connecting the two regimes, where particular points that will later be discussed are highlighted.

Next, we assess the effect of the potential in Eq. (2) on the stability of these new solutions. Starting from the different stationary solutions in Fig. 2**a.** denoted by roman numerals $(i) - (viii)$. We follow the

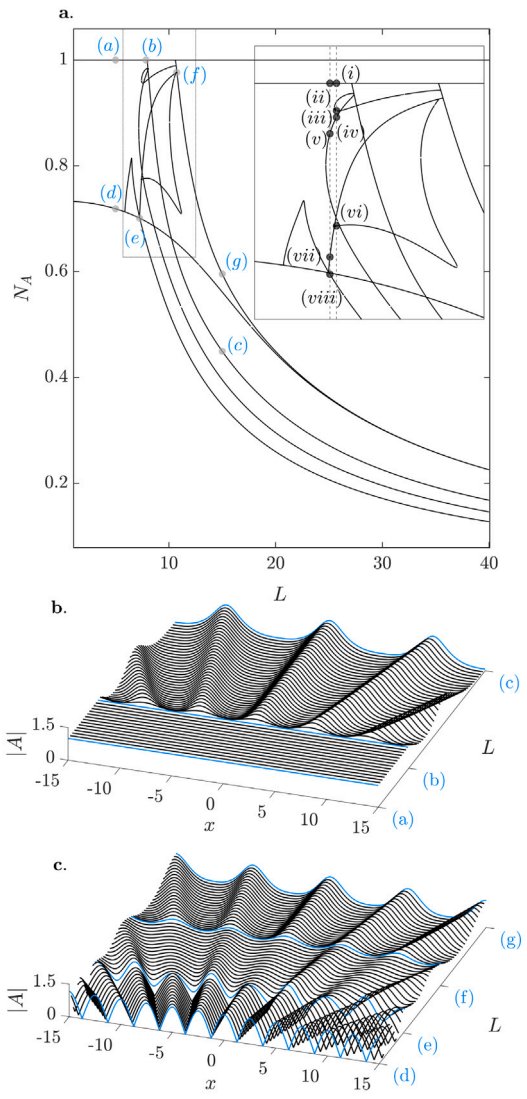

Fig. 2. Selected families of solutions of the unmodulated system. **a.** Branches of different stationary solutions of the CGLE. Inset shows a zoom of the branches that connect different states. The points denoted by roman numerals are later discussed in Fig. 3. **b.** Spatial amplitude profile of the solutions as a function of the spatial period L, starting by the homogeneous solution, point labelled as (a) in the right axis, and following by points labelled by (b) and (c), previously indicated in figure **a. c.** Amplitude of the solutions, varying L and following the branches, starting at point (d) and following the path (e), (f) and (g) in figure **a.** Note that all solutions are unstable.

branches of every solution by scanning the potential amplitude, m, for a fixed value of the phase, ϕ, and for two different values of L, aligned with dashed lines in Fig. 2a. Their corresponding growth rate is provided in Fig. 3**b.** and 3**c.**. Note that, in accordance to Fig. 1**c.**, the growth rate of the modulated homogeneous solution is in general reduced increasing m, see points (i) and (ii) in Fig. 3. However, as above mentioned, modulating the homogeneous solutions does not lead to stabilisation because this solution disappears in a SN bifurcation with another solution already existing in the unmodulated system. Thus, our aim is to find other solutions to be stabilised. Note that these two points are visually overlapped since the modulation is very small.

Interestingly, among the rich turbulent dynamics of the unmodulated CGLE we unveil families of unstable solutions that eventually achieve full stabilisation driven by the non-Hermitian potential. Such stabilised solutions do not evolve directly from the homogeneous solution but from other preexisting solutions of the unmodulated system, see the ranges marked with a thicker black line in Fig. 3**a.**

The profiles of the solutions for weak modulations are provided in Fig. 3 $(i) - (viii)$. As already mentioned, (i) and (ii) correspond to the weakly modulated homogeneous solution. In accordance, we can observe the appearance of harmonics of the potential modulation with very small amplitude. For $L = 15$, the stabilised solution emerges from the unmodulated solution (iii) in Fig. 2**a.** The modulated homogeneous solution (i) and (ii) experience a SN with solutions (iv) and (v) that come from the same solution solutions since they are in the same branch in Fig. 2**a.** Note that this is not true for all values of L since the branch of the solution of (iv) and (v) does not exist for all L.

We can observe the difference between solution (vi) and (vii), both near the same bifurcation point but in different branches and showing different periods, *i.e.* solution (vii) has a double period. In the same way, apart from the discussed solutions of period L, we find many other solutions with period nL, although their detailed analysis may be addressed in another work.

From the stable solution for $L = 15$ and smoothly scanning the period L, we can find the stable range for a periodicity $L = 14.6$ and follow its branch by scanning the modulation amplitude m. Note that this stable solution does not emerge from the same branches of unmodulated solutions as for $L = 15$. See points (iii), (vi) and (vii), and $(viii)$ in Fig. 3**a.**

Focusing the study on this particular stable solution, we determine the stability ranges in the modulation parameter space (m, ϕ, L) to assess the robustness of the proposal. We follow the proposed stable solution to build the stability charts for different periodicities L, mapped in the (m, ϕ) plane. We restrict the values of the modulation amplitude avoiding local losses, *i.e.* for a value of m lower than the homogeneous normalised gain ($m < 1$). The results are presented in Fig. 4, showing extended stabilisation areas for a wide range of periodicities. We observe that such areas shrink above and below the optimised ranges of L up to disappear for $m < 1$. Moreover, we note that stabilisation is found even for very tiny modulations of gain and refractive index, up to only a 5% modulation amplitude for some cases. Two different cases can be differentiated, *i.e.* in-phase and anti-phased real and imaginary parts of the complex potential. In the in-phase case, for $0 < \phi < \pi/2$, stability extends from small to large values of m and ϕ values from 0.5 to 1. In the anti-phase case, for $\pi/2 < \phi < \pi$, stabilisation is found even for lower amplitude values for selected periodicities. The robustness and high efficiency of the stabilisation scheme has also been numerically checked by direct propagation of the solution with a random noise. Moreover, the system tends to this stable solution from the MI of the homogeneous state.

Increasing the spatial periodicity L for fixed values of m and ϕ, stability reappears in isolated areas that open and close by Saddle–Node bifurcations. The stable solution becomes continuous for large enough values of L, *i.e.* for infinitely extended systems and systems with periodic boundary conditions with large enough periodicities. We depict four different branches, as an example in Fig. 5. From lower to higher values of L we first find a closed loop that corresponds to the solution that we previously studied, see solution (i). in accordance with previous results of Fig. 4 we see no stability for this pair of parameters. In addition, we find a stable branch that evolves either towards a unstable Localised Solution (LS) over a zero background, on one side, or generates non-isolated loop-like branch. A particular stable state is shown in panel (ii). We also find a simple branch isolated by two SN. A zoom of this branch is shown in the inset and the solution for a particular L value is plotted in (iii). Last, when increasing L we find a big area of stability. For this case we also provide a zoom of the branch and two different solutions of this branch, (iv) and (v). Inspecting the solutions of the different panels we can recognise that the solutions may arise from a snake bifurcation structure with the number of ripples increasing between branches.

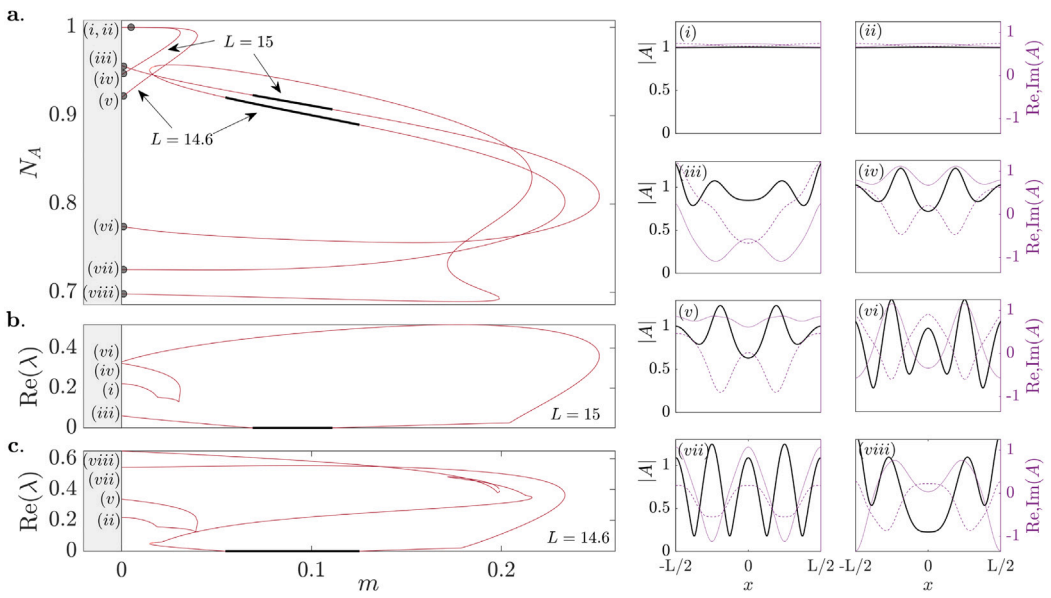

Fig. 3. Selected families of solutions of the modulated system. **a.** Norm vs. modulation amplitude m with fixed $\phi = 2$. Thicker black lines correspond to stable solutions. The spatial profile of the field of the points labelled $(i)-(viii)$, is provided in the corresponding separate panels, where the solid-dashed–dotted lines correspond to absolute value-real part-imaginary part. **b.** and **c.** Maximum growth rate for the solutions in **a.** for different periodicity $L = 15$ and $L = 14.6$. The labels $(i)-(viii)$ correspond to the modulated solutions deriving from $(i)-(viii)$ in Fig. 2**a**.

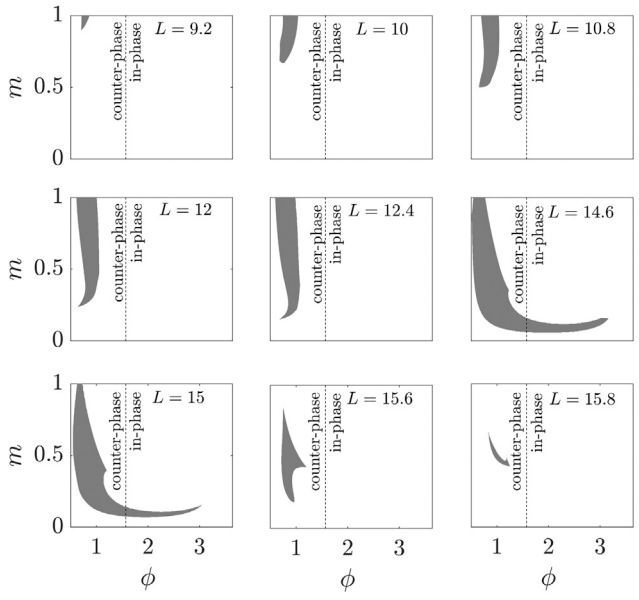

Fig. 4. Stability chart for the family of solutions in the modulation amplitude, phase plane (ϕ, m). These different panels indicate the stability region of the same solution for different values of the periodicity L.

Trivially, analogous stabilisation results may be proven for smaller values of the self-focusing coefficient but also for higher ones, corresponding to less and more unstable situations, respectively. This is shown in Fig. 6, where all three diagrams corresponding to different L values and fixed m and ϕ values, show stable solutions. We observe that stable solutions appear for smaller L values when α is increased. This may be attributed to the fact that for higher values of α, the unstable wavevector range of the CGLE is larger, $0 < k_{uns}^2 < 2\alpha$, see [43], and stable solutions with a smaller period are found. Keeping in mind that the coupling vector of the potential is $q = \pi/L$ hints that is plausible that L must decrease. We show three examples of stable solutions in panels $(i) - (iii)$. These three solutions are connected through the parameter space.

2.1. Generality of the proposal

First, we can generalise the CGLE to its fractional counterpart, that consider different diffraction laws. Recently, fractional versions of some of the most universal equations are attracting interest. This is the case for the Fractional Schrödinger and Fractional Ginzburg–Landau equation that have been studied in mathematics [44,45], finding also its applications in physics [46–49]. The Fractional Complex Ginzburg Landau Equation (FCGLE) can be written in the following form:

$$\frac{\partial A}{\partial t} = (1 - i\alpha)\left(1 - |A|^2\right) A + (i + d)\left(\nabla^2\right)^{\frac{\beta}{2}} A + V(\mathbf{r}, t)A, \tag{3}$$

where the fractional derivative is defined as the integral operator by the Fourier Transform:

$$\left(-\nabla^2\right)^{\frac{\beta}{2}} A = \frac{1}{2\pi} \iint d\mathbf{k} d\mathbf{r}' \, |\mathbf{k}|^{\beta} \exp\left[i\mathbf{k}\left(\mathbf{r} - \mathbf{r}'\right)\right] A\left(\mathbf{r}'\right). \tag{4}$$

We have checked the effect of the potential for different values of β corresponding to different dispersion laws. We found stable solutions for fixed values of the parameters of the potential. In Fig. 7 we show different profiles of stable states for different fractional orders. We see that we can stabilise two different families of solutions, for instance states $(i) - (iii)$ and $(iv) - (vi)$. Although we have not been able to find stable solutions in between for $1.3 \gtrsim \beta \lesssim 1.75$ by direct propagation, maybe both solutions are connected through several SN. The study of the branch structure of the system would correspond to another work.

We can also extend the proposal to higher dimensions using the same fundamental equation, the CGLE but in a 2D space, and second we apply it to a laser system that not only involves a unique field but also a second extended variable, the density of the carrier inversion.

In the 2D case, the potential is the one considered in the unidimensional case applied to both spatial directions and can be written as $V(x, y) = V(x) + V(y)$. In an analogue manner, such a potential stabilises already existing solutions or creates new stable ones that are easily excited via MI. see Fig. 8. A more exhaustive study for the 2D case could be addressed in another work, although the study of the 1D case gives us a very good glimpse on the stabilising behaviour for two spatial dimensions.

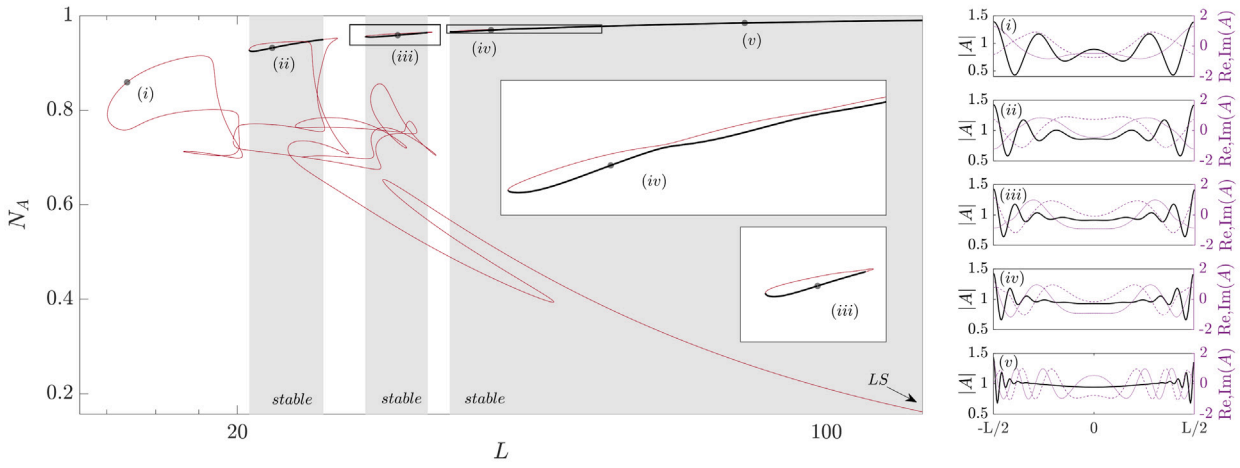

Fig. 5. Periodic solutions as a function of the potential periodicity L. Branches of different solutions of the modulated system with $m = 0.2$ and $\phi = 2$. The spatial profile of the field of the points labelled $(i) - (viii)$, is provided in the corresponding separate panels, where the solid-dashed–dotted lines correspond to absolute value-real part-imaginary part.

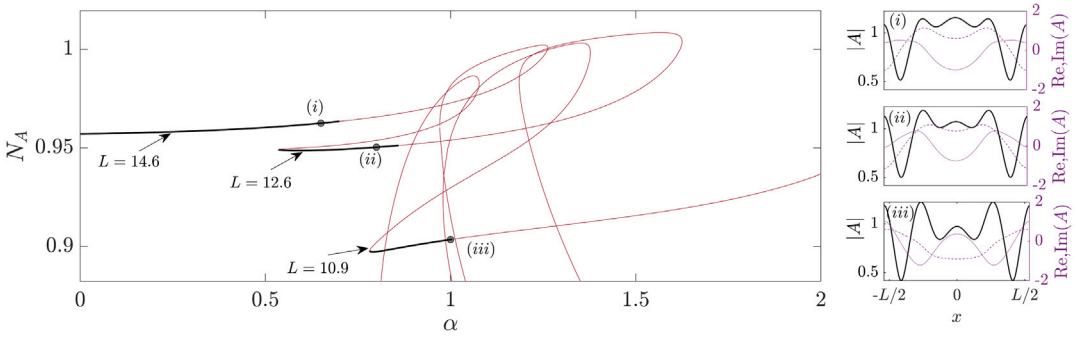

Fig. 6. Periodic solutions as a function of the Self-focusing parameter. Branches of different stable solutions of the modulated system with $m = 0.7$ and $\phi = 0.7$. The spatial profile of the field of the points labelled $(i) - (iii)$, is provided in the corresponding separate panels, where the solid/dashed/dotted lines correspond to absolute value/real part/imaginary part.

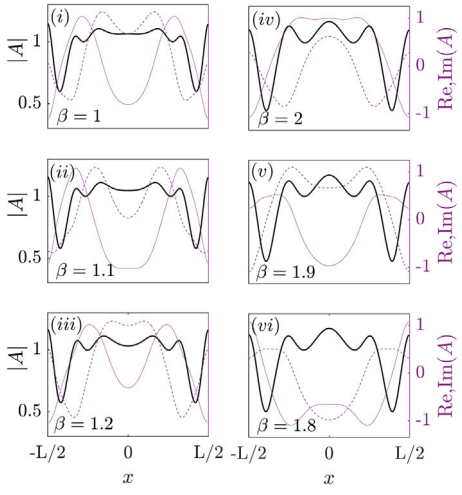

Fig. 7. Spatial field profiles of stable solution for different β values. Solid-dashed–dotted lines correspond to absolute value-real part-imaginary part. (i): $\beta = 1$. (ii): $\beta = 1.1$. (iii): $\beta = 1.2$. (iv): $\beta = 2$. (v): $\beta = 1.9$. (vi): $\beta = 1.8$. $L = 14.8$, $m = 0.7$ and $\phi = 0.8$ for all panels.

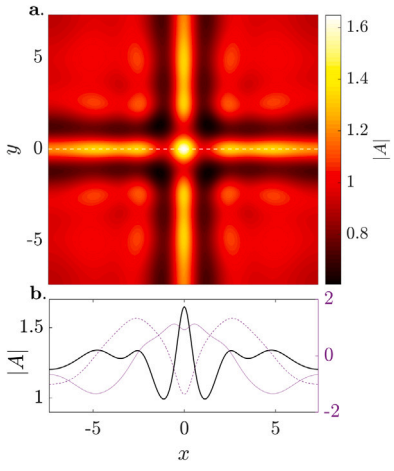

Fig. 8. Stable solution for the 2D CGLE. **a.** Absolute value of a stable field in 2D for $m = 0.4$, $\phi = 0.85 + \pi$ **b.** Cross section at $y = 0$ with similar structure as the one found in the modulated 1D CGLE system. $\alpha = 0.7$.

The dynamics of VCSELs can be described in a simple approximation by the CGLE when only the electromagnetic field is considered. However, the model is only useful for particular cases when VCSELs act as class A lasers. A more physical model of these devices should contain equations for both, field and population inversion of carriers, the carrier density. The model corresponds to class B lasers with higher instability.

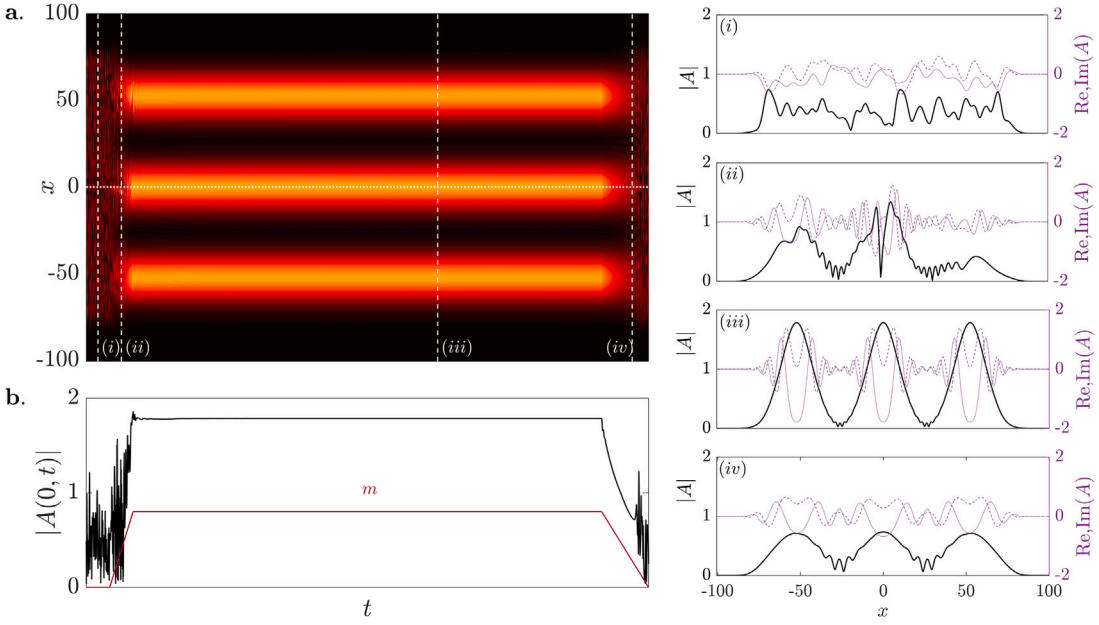

Fig. 9. **a.** Transient evolution of the field profile from a turbulent state of the autonomous system to the stable stationary state when the potential is applied and its destabilisation when the potential is removed. **b.** Temporal evolution of the central point ($x = 0$) and potential amplitude, m, applied. Panels correspond to snapshots of the field profile intensity, real and imaginary parts of the field at different temporal instants showing (i) turbulence (ii) transition to stabilisation, (iii) stable state and (iv), transition to the turbulent state. $\theta = -2$, $C = 0.6$, $\alpha = 2$, $\gamma = 0.01$, $I_p = 2$ and $d = 0.052$.

The temporal evolution of field and carriers may be described as:

$$\begin{aligned}\frac{\partial E}{\partial t} &= -\left[1 + i\theta + 2C\left(i\alpha - 1\right)\left(N - 1\right)\right]E + i\nabla_{\perp}^{2}E + V(\mathbf{r}) \\ \frac{\partial N}{\partial t} &= -\gamma\left[N - I_p + |E|^2\left(N - 1\right)\right] + \gamma d\nabla_{\perp}^{2}N\end{aligned} \tag{5}$$

Assuming V as described in Eq. (2) for a finite-size laser with boundary contours given by and hipergaussian function, a big region in parameter space with a stable solution is found. For such parameters the system stabilises in a short period of time with the introduction of the potential, while it behaves in a turbulent manner without it, see Fig. 9. Note the fast temporal evolution of the field towards the final stable state when switching on the potential and its return to the turbulent state when turning off the potential.

3. Conclusions

We have uncovered new families of periodic solutions of the CGLE which stabilisation may be triggered via the introduction of a stationary periodic non-Hermitian potential. We prove that such potential can stabilise the system by creating an attractor basin for almost any periodicity. A comprehensive analysis is performed on the 1D CGLE showing this effect is robust and efficient, achieving stabilisation for a wide range of parameters even for a small modulation. The results are then extended to 2D systems governed by the CGLE and to the fractional CGLE. Moreover, the proposal holds also for Ginzburglike models describing actual systems, for instance a 1D VCEL. According to the universal character of the CGLE, we expect the present study to be useful to avoid turbulent regimes in different physical systems, among which lasers.

4. Numerical methods

4.1. Stationary solutions

Our purpose is to find stable solutions of Eq. (1) to prevent the system from entering into a turbulent state, which is the case for the unmodulated problem. This stable states must be, at least, stationary solutions. These solutions are sought by numerically solving the model. We look for solutions of the form $A(\mathbf{r},t) = A(\mathbf{r})\exp(i\omega t)$ where ω corresponds to its characteristic frequency. Following [42], this leads to:

$$\begin{aligned}0 \equiv\ & M(A,\omega) = (i+d)\nabla^2 A + \\ & + (1 - i\alpha)\left(1 - |A|^2\right)A + V(\mathbf{r})A - i\omega A.\end{aligned} \tag{6}$$

Using a modified Newton method to solve Eq. (6). In order to do this we may considering a close guess $\{\bar{A},\bar{\omega}\}$ of the solution $\{A,\omega\}$. We can get linearised equations for the correction $\{\delta A,\delta\omega\}$ of the guess:

$$\mathbf{0} = \begin{bmatrix} M' \\ M'' \end{bmatrix} + \begin{bmatrix} B_- & C_- \\ C_+ & B_- \end{bmatrix}\begin{bmatrix} \delta A' \\ \delta A'' \end{bmatrix} + \delta\omega\begin{bmatrix} C \\ D \end{bmatrix}, \tag{7}$$

where $B_{\pm} \equiv d\nabla^2 + 1 - 2\left|\bar{A}\right|^2 + V' \pm \left(\bar{A}'^2 - \bar{A}''^2\right)$, $C_{\pm} \equiv -2A'A'' \pm \left(\nabla^2 - \alpha + V'' + \omega\right)$, $D \equiv -A''$ and $E \equiv A'$. Superscripts ' and " correspond to real and imaginary parts. The solution is solved by correcting the guess at each iteration with the calculated corrections $\{\delta A,\delta\omega\}$ until $M\left(\bar{A},\bar{\omega}\right) = 0$ for a given precision. One can clearly see that the system from Eq. (7) is undetermined since we have one extra unknown. Numerically, the system has $2N_xN_y$ equations. Here N_x and N_y correspond to the number of points we take in x and y. Since the guess solution that we introduce is close to the solution one can fix the field A at one point and so, the correction δA will be zero at that point, reducing one unknown. So for that equation one can calculate $\delta\omega$ and then use this correction of the propagation constant to calculate the rest of corrections.

4.2. Linear stability analysis

In order to study the stability analysis of the stationary solutions we consider the standard linear stability. To do this we consider a small perturbation of the stationary state $A = \bar{A}(x,\omega) + ae^{\lambda t} + b^*e^{\lambda^* t}$. Where $\bar{A}(x,\omega)$ is the stationary solution and a and b are the small perturbation eigenfunctions ($|a|, |b| \ll |\bar{A}|$) and the real part of the Lyapunov exponents, λ determine the stability. Substituting the perturbed state into Eq. (1) we obtain a linear eigenvalue problem that be solved numerically. Stability of the solutions is also tested by direct propagation.

CRediT authorship contribution statement

Salim B. Ivars: Software, Data curation, Validation, Writing – review & editing. **Muriel Botey:** Supervision, Validation, Writing – review & editing. **Ramon Herrero:** Conceptualization, Supervision, Validation, Writing – review & editing. **Kestutis Staliunas:** Conceptualization, Supervision, Validation, Writing – review & editing.

Declaration of competing interest

The authors declare that they have no known competing financial interests or personal relationships that could have appeared to influence the work reported in this paper.

Data availability

No data was used for the research described in the article.

Acknowledgements

This work was supported by the Government of Spain through grants IJCI-2016-27752, MTM2016-75963-P, FIS2015-71559-P and Severo Ochoa CEX2019-000910-S; Generalitat de Catalunya, Spain; CERCA, Spain; Fundació Cellex, Spain; and Fundació Mir-Puig, Spain. K.S acknowledges European Social Fund (project No 09.3.3- LMT-K712-17- 0016) under grant agreement with the Research Council of Lithuania (LMTLT).

References

[1] Aranson IS, Kramer L. The world of the complex Ginzburg-Landau equation. Rev Modern Phys 2002;74(1):99.
[2] Collet P. Thermodynamic limit of the Ginzburg-Landau equations. Nonlinearity 1994;7(4):1175.
[3] Akhmediev N, Ankiewicz A, Soto-Crespo J. Multisoliton solutions of the complex Ginzburg-Landau equation. Phys Rev Lett 1997;79(21):4047.
[4] Osman M, Ghanbari B, Machado J. New complex waves in nonlinear optics based on the complex Ginzburg-Landau equation with Kerr law nonlinearity. Eur Phys J Plus 2019;134(1):1–10.
[5] Scheuer J, Malomed BA. Stable and chaotic solutions of the complex Ginzburg–Landau equation with periodic boundary conditions. Physica D 2002;161(1–2):102–15.
[6] Columbo L, Piccardo M, Prati F, Lugiato L, Brambilla M, Gatti A, Silvestri C, Gioannini M, Opačak N, Schwarz B, et al. Unifying frequency combs in active and passive cavities: Temporal solitons in externally driven ring lasers. Phys Rev Lett 2021;126(17):173903.
[7] Staliunas K, Sanchez-Morcillo VJ. Transverse patterns in nonlinear optical resonators, vol. 183. Springer Science & Business Media; 2003.
[8] Tasbozan O, Kurt A, Tozar A. New optical solutions of complex Ginzburg–Landau equation arising in semiconductor lasers. Appl Phys B 2019;125(6):1–12.
[9] Akhmediev N, Soto-Crespo JM, Town G. Pulsating solitons, chaotic solitons, period doubling, and pulse coexistence in mode-locked lasers: Complex Ginzburg-Landau equation approach. Phys Rev E 2001;63(5):056602.
[10] Li W, Ma G, Yu W, Zhang Y, Liu M, Yang C, Liu W. Soliton structures in the (1+ 1)-dimensional Ginzburg–Landau equation with a parity-time-symmetric potential in ultrafast optics. Chin Phys B 2018;27(3):030504.
[11] Akhmediev N, Ankiewicz A, Soto-Crespo J. Stable soliton pairs in optical transmission lines and fiber lasers. J Opt Soc Amer B 1998;15(2):515–23.
[12] Sakaguchi H. Hole solutions in the complex Ginzburg-Landau equation near a subcritical bifurcation. Progr Theoret Phys 1991;86(1):7–12.
[13] Deissler RJ, Brand HR. Periodic, quasiperiodic, and chaotic localized solutions of the quintic complex Ginzburg-Landau equation. Phys Rev Lett 1994;72(4):478.
[14] Afanasjev V, Akhmediev N, Soto-Crespo J. Three forms of localized solutions of the quintic complex Ginzburg-Landau equation. Phys Rev E 1996;53(2):1931.
[15] Carvalho M, Facao M. Dissipative solitons for generalizations of the cubic complex Ginzburg-Landau equation. Phys Rev E 2019;100(3):032222.
[16] López V, Boyland P, Heath MT, Moser RD. Relative periodic solutions of the complex Ginzburg–Landau equation. SIAM J Appl Dyn Syst 2005;4(4):1042–75.
[17] Porubov A, Velarde M. Exact periodic solutions of the complex Ginzburg–Landau equation. J Math Phys 1999;40(2):884–96.
[18] Kochetov BA, Tuz VR. Replication of dissipative vortices modeled by the complex Ginzburg-Landau equation. Phys Rev E 2018;98(6):062214.
[19] Skryabin DV, Vladimirov AG. Vortex induced rotation of clusters of localized states in the complex Ginzburg-Landau equation. Phys Rev Lett 2002;89(4):044101.
[20] Coullet P, Gil L, Rocca F. Optical vortices. Opt Commun 1989;73(5):403–8.
[21] Weiss C, Vaupel M, Staliunas K, Slekys G, Taranenko V. Solitons and vortices in lasers. Appl Phys B 1999;68(2):151–68.
[22] Isah MA, Yokuş A. The investigation of several soliton solutions to the complex Ginzburg-Landau model with Kerr law nonlinearity. Math Model Numer Simul Appl 2022;2(3):147–63.
[23] Malomed BA. New findings for the old problem: Exact solutions for domain walls in coupled real Ginzburg-Landau equations. Phys Lett A 2022;422:127802.
[24] Zafar A, Shakeel M, Ali A, Akinyemi L, Rezazadeh H. Optical solitons of nonlinear complex Ginzburg–Landau equation via two modified expansion schemes. Opt Quantum Electron 2022;54(1):1–15.
[25] Facao M, Carvalho MI. Existence and stability of solutions of the cubic complex Ginzburg-Landau equation with delayed Raman scattering. Phys Rev E 2015;92(2):022922.
[26] Sakaguchi H, Skryabin DV, Malomed BA. Stationary and oscillatory bound states of dissipative solitons created by third-order dispersion. Opt Lett 2018;43(11):2688–91.
[27] Mayteevarunyoo T, Malomed BA, Skryabin DV. One-and two-dimensional modes in the complex Ginzburg-Landau equation with a trapping potential. Opt Express 2018;26(7):8849–65.
[28] Chaté H, Manneville P. Phase diagram of the two-dimensional complex Ginzburg-Landau equation. Physica A: Statist. Mech. Appl. 1996;224(1–2):348–68.
[29] Falkovich G, Gawdzki K, Vergassola M. Particles and fields in fluid turbulence. Rev Modern Phys 2001;73(4):913.
[30] Ikeda K, Daido H, Akimoto O. Optical turbulence: chaotic behavior of transmitted light from a ring cavity. Phys Rev Lett 1980;45(9):709.
[31] Hess O, Koch SW, Moloney JV. Filamentation and beam propagation in broad-area semiconductor lasers. IEEE J Quantum Electron 1995;31(1):35–43.
[32] Battogtokh D, Mikhailov A. Controlling turbulence in the complex Ginzburg-Landau equation. Physica D 1996;90(1–2):84–95.
[33] Xiao J, Hu G, Yang J, Gao J. Controlling turbulence in the complex Ginzburg-Landau equation. Phys Rev Lett 1998;81(25):5552.
[34] Kumar S, Herrero R, Botey M, Staliunas K. Taming of modulation instability by spatio-temporal modulation of the potential. Sci Rep 2015;5(1):1–7.
[35] Bender CM, Boettcher S. Real spectra in non-hermitian Hamiltonians having PT symmetry. Phys Rev Lett 1998;80(24):5243.
[36] Feng L, El-Ganainy R, Ge L. Non-Hermitian photonics based on parity–time symmetry. Nat Photon 2017;11(12):752–62.
[37] El-Ganainy R, Makris KG, Khajavikhan M, Musslimani ZH, Rotter S, Christodoulides DN. Non-Hermitian physics and PT symmetry. Nat Phys 2018;14(1):11–9.
[38] Parto M, Liu YG, Bahari B, Khajavikhan M, Christodoulides DN. Non-Hermitian and topological photonics: optics at an exceptional point. Nanophotonics 2021;10(1):403–23.
[39] Ivars SB, Botey M, Herrero R, Staliunas K. Optical turbulence control by non-hermitian potentials. Phys Rev A 2022;105(3):033510.
[40] Liu B, Li L, Malomed BA. Effects of the third-order dispersion on continuous waves in complex potentials. Eur Phys J D 2017;71(6):1–8.
[41] Driben R, Malomed B. Stabilization of solitons in PT models with supersymmetry by periodic management. Europhys Lett 2011;96(5):51001.
[42] Milián C, Kartashov YV, Skryabin DV, Torner L. Clusters of cavity solitons bounded by conical radiation. Phys Rev Lett 2018;121(10):103903.
[43] Kumar S. Suppression and control of modulation instability. Universitat Politècnica de Catalunya; 2017.
[44] Laskin N. Fractional quantum mechanics and Lévy path integrals. Phys Lett A 2000;268(4–6):298–305.
[45] Weitzner H, Zaslavsky G. Some applications of fractional equations. Commun Nonlinear Sci Numer Simul 2003;8(3–4):273–81.
[46] Herrmann R. Fractional calculus: An introduction for physicists. World Scientific; 2011.
[47] Guo X, Xu M. Some physical applications of fractional Schrödinger equation. J Math Phys 2006;47(8):082104.
[48] Qiu Y, Malomed BA, Mihalache D, Zhu X, Zhang L, He Y. Soliton dynamics in a fractional complex Ginzburg-Landau model. Chaos Solitons Fractals 2020;131:109471.
[49] Tarasov VE, Zaslavsky GM. Fractional Ginzburg–Landau equation for fractal media. Physica A: Statist. Mech. Appl. 2005;354:249–61.